INSTITUT NATIONAL DE RECHERCHE EN INFORMATIQUE ET EN AUTOMATIQUE

A vectorial Matching Pursuit algorithm with an application to the analysis of Vecto-cardiogram signals

Catherine Bonnet , Jonathan R. Partington , Michel Sorine

N ° 4535

Septembre 2002

THÈME 4

ISSN 0249-6399 ISRN INRIA/RR--4535--FR

INRIA
ROCQUENCOURT

A vectorial Matching Pursuit algorithm with an application to the analysis of Vecto-cardiogram signals

Catherine Bonnet , Jonathan R. Partington * , Michel Sorine

Thème 4 — Simulation et optimisation
de systèmes complexes
Projet Sosso

Rapport de recherche n ° 4535 — septembre 2002 — 14 pages

Abstract: A modification of the Matching Pursuit algorithm is presented which allows the recovery of a vector-valued signal from partial data (a relaxed version of the algorithm is also introduced, and shown to converge). The new algorithm is illustrated by its application to the analysis of a vecto-cardiogram signal.

Key-words: vectorial matching pursuit algorithm, relaxed matching pursuit algorithm, vector-valued signal, vecto-cardiogram signal

(Résumé : tsvp)

* Department of Mathematics, University of Leeds, Leeds LS29JT, U.K

Un algorithme de Matching Pursuit vectoriel et une application à l'analyse de signaux vecto-cardiographiques

Résumé : Nous présentons une modification de l'algorithme de matching pursuit permettant la reconstruction d'un signal vectoriel (une version relaxée de cet algorithme est également introduite et il est prouvé qu'elle converge). Ce nouvel algorithme est illustré par une application à l'analyse d'un signal vecto-cardiographique.

Mots-clé : algorithme de matching pursuit vectoriel, algorithme de matching pursuit relaxé, signal vectoriel, signal vecto-cardiographique

1 Introduction

The Matching Pursuit algorithm [10, 7, 12, 5] is an algorithm that has been used in such settings as signal and image processing when one has large amounts of information available from which one must select the most important features. This enables one to obtain a more easily-analysed approximation to the given data. Versions of this algorithm have also been used in medical contexts for the analysis of breathing rhythms [1] and brain patterns [8].

In this paper we present two refinements of the algorithm. One is a *relaxed* version which in some situations leads to faster convergence. The other refinement allows us to handle vector-valued data, and this is illustrated by an application to the analysis of vecto-cardiogram (VCG) data. Other techniques have been applied to the analysis of scalar-valued (ECG) data, and we mention the papers [2, 4, 6] for general background information.

In Section 2 we present the mathematical basis of the modified Matching Pursuit algorithm, and in Section 3 we see how this can be applied to signal processing. Section 4 contains the numerical example, illustrating the technique and highlighting the use of vectorial data (compared with the standard scalar data) in the analysis of cardiac frequency.

2 The Matching Pursuit Algorithm

2.1 The basic algorithm

The standard Matching Pursuit algorithm, as given in [10, 5], allows one to construct approximations to an element of a Hilbert space H using vectors from a fixed set. In the notation of [12, Sec. 5.2], we are supplied with a *dictionary* of normalized vectors, $\{g_\alpha \in H : \alpha \in A\}$ and an element f of H. For computational purposes, A is normally finite, but this is not theoretically necessary. We fix γ with $0 < \gamma < 1$ and set $f_0 = f$. For each $n \geq 0$ we inductively choose $\alpha_n \in A$ such that

$$|\langle f_n, g_{\alpha_n}\rangle| \geq \gamma \sup_{\alpha \in A} |\langle f_n, g_\alpha\rangle|, \tag{1}$$

and we set

$$f_n = \langle f_n, g_{\alpha_n}\rangle g_{\alpha_n} + f_{n+1} := h_n + f_{n+1}, \tag{2}$$

say. Then it is the case that $h_0 + h_1 + \ldots$ converges in norm to the orthogonal projection of f onto the closed linear span of the dictionary elements.

Note that, if the dictionary is an orthonormal basis, then the expansion produced by the Matching Pursuit algorithm is a standard orthonormal expansion, in (approximately) decreasing order of coefficients.

2.2 A relaxed algorithm

We may modify the Matching Pursuit algorithm, by replacing the iteration (2) by

$$f_n = \lambda\langle f_n, g_{\alpha_n}\rangle g_{\alpha_n} + f_{n+1} := h_n + f_{n+1}, \tag{3}$$

where λ is chosen to lie between 0 and 2. One can also make λ depend on n, provided that the sequence of values does not accumulate near 0 or 2, but we shall treat only the simpler case. This idea

is well-known in Numerical Analysis under the name of *relaxation* (see, for example, [3]). Although this modified algorithm is definitely suboptimal if the dictionary vectors are orthonormal, it can lead to faster convergence in some other circumstances, for example for the slowly converging example $H = \mathbb{R}^2$, $f = (0,1)$, $A = \{1,2\}$, $g_1 = (1,0)$, $g_2 = (\cos\delta, \sin\delta)$, with $\delta > 0$ (small), given in [7]. Some computational experience suggests that a value of λ of about 1.2 can be quite effective.

Theorem 2.1 *In the relaxed Matching Pursuit algorithm given by the iteration (3) the sequence (f_n) converges in norm to the orthogonal projection of f onto the closed linear span of the dictionary.*

Proof. This is a fairly straightforward modification of the proof for the case $\lambda = 1$ given in [10]; we are using the same notation as in [12]. First, it is easy to see that we may assume without loss of generality that the closed linear span of the dictionary is the whole of H, since vectors orthogonal to the dictionary play no part in the algorithm. Next, we have

$$f_{n+1} = f_n - \lambda \langle f_n, g_{\alpha_n} \rangle g_{\alpha_n}, \tag{4}$$

so that

$$\begin{aligned} \|f_{n+1}\|^2 &= \|f_n\|^2 - 2\lambda |\langle f_n, g_{\alpha_n}\rangle|^2 + \lambda^2 |\langle f_n, g_{\alpha_n}\rangle|^2 \\ &= \|f_n\|^2 + (\lambda^2 - 2\lambda)|\langle f_n, g_{\alpha_n}\rangle|^2 \leq \|f_n\|^2, \end{aligned} \tag{5}$$

since $0 < \lambda < 2$. Let $m > n$ and write $f_m = f_n - \sum_{k=n}^{m-1} h_k$, so that

$$\begin{aligned} \|f_n - f_m\|^2 &= \langle f_n - f_m, f_n \rangle - \langle f_n - f_m, f_m \rangle \\ &= \langle f_n, f_n \rangle - \langle f_m, f_n - f_m + f_m \rangle - \langle f_n - f_m, f_m \rangle \\ &= \|f_n\|^2 - \|f_m\|^2 - 2\,\mathrm{Re}\langle f_m, f_n - f_m \rangle \\ &= \|f_n\|^2 - \|f_m\|^2 - 2\,\mathrm{Re}\langle f_m, \sum_{k=n}^{m-1} h_k \rangle. \end{aligned} \tag{6}$$

Now

$$\left| \langle \sum_{k=n}^{m-1} h_k, f_m \rangle \right| \leq \sum_{k=n}^{m-1} \lambda |\langle f_k, g_{\alpha_k}\rangle|\, |\langle g_{\alpha_k}, f_m \rangle| \leq \sum_{k=n}^{m-1} \|h_k\|\, \|h_m\| / (\lambda\gamma). \tag{7}$$

Also

$$\|h_k\|^2 = \lambda^2 |\langle f_k, g_{\alpha_k}\rangle|^2 = \frac{\lambda^2}{2\lambda - \lambda^2} (\|f_k\|^2 - \|f_{k+1}\|^2), \tag{8}$$

by (5), and hence $C^2 := \sum_{k=1}^{\infty} \|h_k\|^2 < \infty$. Hence, for each $\epsilon > 0$, it is the case that

$$\|h_m\| \leq \epsilon / \sqrt{m} \tag{9}$$

for infinitely many m. Now, by the Cauchy–Schwarz inequality,

$$\sum_{k=n}^{m-1} \|h_k\| \leq \sqrt{m-n} \left(\sum_{k=n}^{m-1} \|h_k\|^2 \right)^{1/2} \leq C\sqrt{m}, \tag{10}$$

for all $m > n$. Finally

$$\|f_n - f_m\|^2 \leq \|f_n\|^2 - \|f_m\|^2 + 2(C\sqrt{m})(\epsilon/\sqrt{m})/(\lambda\gamma), \tag{11}$$

for infinitely many m and all $n < m$, by (6), (7), (10) and (9), which implies that (f_n) is a Cauchy sequence. We now observe that (f_n), being a bounded sequence, has a subsequence which tends weakly to a limit, necessarily zero, and hence the norm limit of (f_n) is also zero.

□

2.3 A vectorial version

The Matching Pursuit algorithm, in either its traditional or relaxed form, can also be applied in the situation when the given data is vector-valued. We shall now give a rather abstract formulation of the vectorial algorithm: in Section 3.2 we shall describe how this works in a more concrete situation.

Suppose that we are given a collection of bounded linear operators $\{T_\alpha : H \to K_\alpha : \ \alpha \in A\}$, where each K_α is a Hilbert space. The vectorial algorithm uses the dictionary

$$\{T_\alpha^* k : \ k \in K_\alpha, \ \|T_\alpha^* k\| = 1, \ \alpha \in A\}. \tag{12}$$

Hence we select at each stage an $\alpha_n \in A$ and $k_n \in K_{\alpha_n}$ such that $\|T_{\alpha_n}^* k_n\| = 1$ and the quantity

$$\langle f_n, T_{\alpha_n}^* k_n \rangle = \langle T_{\alpha_n} f_n, k_n \rangle \tag{13}$$

is large. We then define

$$f_{n+1} = f_n - \lambda \langle T_{\alpha_n} f_n, k_n \rangle T_{\alpha_n}^* k_n, \tag{14}$$

starting the iteration with $f_0 = f$.

The computations become simpler when $\|T_\alpha^* k\|$ is a constant multiple of $\|k\|$, independently of α and the choice of $k \in K_\alpha$. In that case, we select $\alpha_n \in A$ such that $\|T_{\alpha_n} f_n\|$ is large, and take

$$k_n = T_{\alpha_n} f_n / \|T_{\alpha_n}^* T_{\alpha_n} f_n\|. \tag{15}$$

Now

$$\begin{aligned} f_{n+1} &= f_n - \lambda \langle f_n, T_{\alpha_n}^* k_n \rangle T_{\alpha_n}^* k_n \\ &= f_n - \lambda \|T_{\alpha_n} f_n\|^2 T_{\alpha_n}^* T_{\alpha_n} f_n / \|T_{\alpha_n}^* T_{\alpha_n} f_n\|^2. \end{aligned} \tag{16}$$

We again obtain norm convergence onto the projection of f onto the closed linear span of the dictionary vectors.

3 Application to Paley–Wiener signals

3.1 The scalar case

We work with the Paley–Wiener space $PW(b)$ of band-limited signals. This consists of all functions having a representation

$$f(t) = \frac{1}{2\pi} \int_{-b}^{b} \hat{f}(x) e^{ixt} \, dx, \tag{17}$$

where $b > 0$ is the *bandwidth*, and $\hat{f} \in L_2[-b, b]$. $\hat{f}$ is the Fourier transform of f. Normally we prefer to work with real-valued signals, in which case we insist also that our functions satisfy $\hat{f}(x) = \overline{\hat{f}(-x)}$. The space $PW(b)$ is a closed subspace of $L_2(\mathbb{R})$, and hence a Hilbert space. A key role is played here by the sinc function, defined by

$$\operatorname{sinc} t = \begin{cases} \frac{\sin t}{t} & \text{if } t \neq 0, \\ 1 & \text{if } t = 0. \end{cases} \tag{18}$$

In particular the Whittaker–Kotel'nikov–Shannon sampling series or cardinal series [9, 12] allows us to recover any $f \in PW(b)$ from regularly-spaced samples, by the formula

$$f(t) = \sum_{n=-\infty}^{\infty} f(n\pi/c) \operatorname{sinc}(ct - n\pi), \tag{19}$$

converging uniformly and in L_2 norm, for any $c \geq b$. Indeed the sequence of functions $\left(\sqrt{\frac{b}{\pi}}\operatorname{sinc}(bt - n\pi)\right)_{n\in\mathbb{Z}}$ forms an orthonormal basis for $PW(b)$; the Fourier transforms of these functions are equal to $\sqrt{\frac{\pi}{b}}e^{-in\pi x/b}$ for $x \in [-b, b]$ and to zero otherwise, and (19) can be derived by expansion in terms of this orthonormal basis.

We take as our dictionary the functions

$$g_\alpha(t) = \sqrt{\frac{b}{\pi}}\operatorname{sinc} b(t - \alpha), \tag{20}$$

where α ranges over the set of sampling points. These functions are normalized, and will even be orthonormal if we make the choice $\alpha_n = n\pi/b$, although this is not necessary for what follows.

Implementation of the matching pursuit algorithm is now extremely easy, because of the standard fact [12] that the sinc function acts as a reproducing kernel, namely

$$\langle f, k_s\rangle = f(s), \qquad \text{for } f \in PW(b), \tag{21}$$

where $k_s(t) = \frac{b}{\pi}\operatorname{sinc} b(t - s)$, for s, $t \in \mathbb{R}$. Hence, given f_n, we obtain f_{n+1} by choosing $\alpha = \alpha_n$ to maximize $|f_n(\alpha)|$ over α in the set of sampling points, and writing

$$f_{n+1} = f_n - \lambda f_n(\alpha_n)\operatorname{sinc} b(t - \alpha_n). \tag{22}$$

In the case $\lambda = 1$ this means that we subtract the multiple of $\operatorname{sinc} b(t - \alpha_n)$ which ensures that f_{n+1} has a zero at α_n.

Our decomposition becomes

$$f(t) \approx \lambda \sum_{n=0}^{N} f_n(\alpha_n)\operatorname{sinc} b(t - \alpha_n), \tag{23}$$

which is a good approximation in the norm of $PW(b)$; in particular, taking Fourier transforms, we have

$$\hat{f}(x) \approx \frac{\lambda\pi}{b}\sum_{n=0}^{N} f_n(\alpha_n)\exp(-i\alpha_n x), \qquad \text{for } |x| < b, \tag{24}$$

which is a good approximation in the norm of $L_2[-b, b]$.

The advantage of this procedure is that we can obtain good estimates of f and $\hat{f}$, even using a small amount of data (e.g. thirty values per second in the VCG example which follows).

3.2 The vector-valued case

In section 2.3 we showed how to apply the Matching Pursuit algorithm in the situation when we have vector-valued data. We now specify to a particular case, when the process is somewhat more intuitive to describe. In the analysis of VCG data we may wish to work with a more general vectorial version of the Paley–Wiener space, which can be written as $PW(b, \mathbb{R}^N)$, for some $N \geq 1$: in our case the value $N = 3$ is appropriate. This space consists of vector-valued functions $f : \mathbb{R} \to \mathbb{R}^N$ given by

$$f(t) = \frac{1}{2\pi}\int_{-b}^{b} \hat{f}(x)e^{ixt}\,dx, \tag{25}$$

where $b > 0$ is the *bandwidth*, and $\hat{f} \in L_2([-b, b], \mathbb{C}^N)$, satisfying $\hat{f}(x) = \overline{\hat{f}(-x)}$ in order that f should be real-valued.

The inner product is now given by

$$\langle f, g\rangle = \int_{\mathbb{R}} f(t)\cdot g(t)\,dt, \tag{26}$$

where $(u,v)\mapsto u\cdot v$ is the usual inner product on $\mathbb{R}^N$.

We now take as our dictionary the infinite set of all functions $g_\alpha \otimes v$, defined by

$$(g_\alpha \otimes v)(t) = g_\alpha(t)v \qquad \text{for } t\in\mathbb{R}, \tag{27}$$

where α is a sampling point, v a unit vector in $\mathbb{R}^N$, and the scalar-valued function g_α as given in (20).

At first sight, implementing the matching pursuit algorithm looks like an intractable numerical problem, since the dictionary is always infinite if $N>1$, but we note that using (21)

$$|\langle f, g_\alpha\otimes v\rangle| = \sqrt{\frac{\pi}{b}}\,|f(\alpha)\cdot v|, \tag{28}$$

so that to maximize $|\langle f, g_\alpha\otimes v\rangle|$ over all α and v is equivalent to the simpler problem of maximizing $\|f(\alpha)\|$ over all the sampling points α and taking $v = f(\alpha)/\|f(\alpha)\|$.

The iterative step of the algorithm thus reads

$$\begin{aligned} f_{n+1}(t) &= f_n(t) - \lambda\langle f, g_{\alpha_n}\otimes v_n\rangle g_{\alpha_n}(t) f_n(\alpha_n)/\|f_n(\alpha_n)\| \\ &= f_n(t) - \lambda f_n(\alpha_n)\,\mathrm{sinc}\,b(t-\alpha_n), \end{aligned} \tag{29}$$

where now $f_n(t)$ and $f_{n+1}(t)$ are vectors in $\mathbb{R}^N$ for each t. Since the algorithm is still a special case of the (relaxed) matching pursuit algorithm, the convergence follows from Theorem 2.1.

4 Analysis of VCG data

We begin with some background on electrocardiography before applying the matching pursuit algorithm to the medical data.

Without going into details, let us just recall that an electrical activity results from heart excitation. While this excitation front progresses through the cardiac muscle, electric potentials of different modulus and directions are created. The equivalent dipole of the heart's electrical activity (see [11]) is the sum vector of these potentials. It varies in length and direction during the excitation cycle, describing a curve in $\mathbb{R}^3$ (the VCG) which might be identified by placing several electrodes on patients at appropriate points in the body. In fact, placing four electrodes will allow one to obtain three signals, which can be considered as being the orthogonal projections of the VCG if the electrodes are suitably placed.

In usual clinical studies, only two electrodes are placed to obtain a single ECG. The analysis of cardiac frequency is actually done from this ECG by identifying the most important peaks of the signal (arising at each heart beat) and constructing the so-called RR interval. The cardiac period is calculated as the mean of the intervals between two peaks.

Obviously, an analysis of the 3D signal should give more information. In particular, compared to a 1D analysis, it should allow an easier detection of small peaks and a better estimation of some inter-peak durations.

To illustrate the method, we work with 1500 data points, each comprising 3 coordinates, which were kindly provided by Dr. Laurence Mangin; these represent 3 seconds' VCG measurements sampled 500 times per second.

Approximation of a signal and its spectrum

It was found convenient to subtract a constant from the data, to give it mean value zero, in order to avoid the behaviour of $\hat{f}$ being dominated by its DC value (the value at 0), but this is not essential. Also the Gram–Schmidt process was used to pre-process the data and make the three channels orthonormal.

Figure 1 represents a one beat VCG and a scalar projection : we can see that the VCG has three main loops with diameters PQ, RS, TU corresponding after projection to the usual peaks of the ECG (P_X, Q_X,R_X, S_X, T_X, U_X). For example, it may be easier to detect P, Q in the VCG than in the ECG allowing easier estimation of the duration of the QT interval (ventricular repolarization).

Figure 2 shows a plot of the full data for the 3 coordinates, and Figure 3 shows a three-dimensional plot of the data.

Figure 4 shows a plot of the full frequency spectrum of the signal (strictly speaking, the pointwise norm of the Fourier transform, which is also vector-valued). This was determined by taking a bandwidth of $b = 500\pi$ and interpolating with the standard cardinal series. Figure 5 shows an enlargement of the low-frequency portion of the spectrum.

Taking a bandwidth of $b = 200$ and $\lambda = 1$ (respectively $\lambda = 0.8$), the approximation produced by 100 iterations of the vectorial (respectively vectorial relaxed) Matching Pursuit algorithm gives a relative vectorial L_2-error norm equal to 0.009 (respectively 0.003) as the approximation produced using the scalar spline algorithm (available in scilab or matlab) on each coordinate on 100 equidistant points among the full data gives a relative error equal to 0.061. Note that if we approximate each coordinate by 100 iterations of the scalar relaxed matching pursuit algorithm with $\lambda = 0.8$, the vectorial L_2 error norm is equal to 0.007 showing then that the vectorial algorithm can improve approximation.

Figure 6–9 are based on the approximation produced by the vectorial relaxed Matching Pursuit algorithm with $\lambda = 0.8$: Figure 6 shows a plot of the vectorial approximation with $\lambda = 0.8$ and Figure 7 shows a three-dimensional plot. Figure 8 shows a plot of the approximated spectrum, and Figure 9 shows a plot of the approximated low-frequency spectrum.

Figure 10 gives the approximation obtained via the scalar spline algorithm.

Acknowledgments

The authors gratefully acknowledge helpful discussions with Julie Bestel and Jean Clairambault.

References

[1] M. Akay and E.J.H. Mulder, Investigating the effect of maternal alcohol intake on human fetal breathing rate using adaptive time-frequency analysis-methods, *Early human develop.* 46 (1996), 153–164.

[2] R.D. Berger, S. Akselrod, D. Gordon and R.J. Cohen, An efficient algorithm for spectral analysis of heart rate variability, *IEEE Trans. Biomed. Eng.* 33 (1986), 900–904.

[3] S.D. Conte and C. De Boor, *Elementary Numerical Analysis*, McGraw–Hill, 3rd Edition (1980).

[4] I. Daskalov and I. Christov, Improvement of resolution in measurement of electrocardiogram RR intervals by interpolation, *Med. Eng. Phys.* 19 (1997), 375–379.

[5] G. Davis, S. Mallat and M. Avellaneda, Adaptive greedy approximations, *Constr. Approx.* 13 (1997), 57–98.

[6] R.W. DeBoer, J.M. Karemaker and J. Strackee, Comparing spectra of a series of point events particularly for heart rate variability data, *IEEE Trans. Biomed. Eng.* 31 (1984), 384–387.

[7] N.F. Dudley Ward and J.R. Partington, Rational wavelet decompositions of transfer functions in Hardy–Sobolev classes, *Math. of Control, Sig. and Sys.* 8 (1995), 257–278.

[8] P.J. Durka and K.J. Blinowska, Analysis of EEG transients by means of matching pursuit, *Ann. Biomed. Eng.* 23 (1995), 608–611.

[9] J.R. Higgins, *Sampling theory in Fourier analysis and signal analysis*, Oxford University Press (1996).

[10] S.G. Mallat and Z.F. Zhang, Matching pursuits with time-frequency dictionaries, *IEEE Trans. Signal Process.* 41 (1993), 3397–3415.

[11] A.V. Panfilov and A.V. Holden (eds.), *Computational biology of the heart*, John Wiley (1996).

[12] J.R. Partington, *Interpolation, identification and sampling*, Oxford University Press (1997).

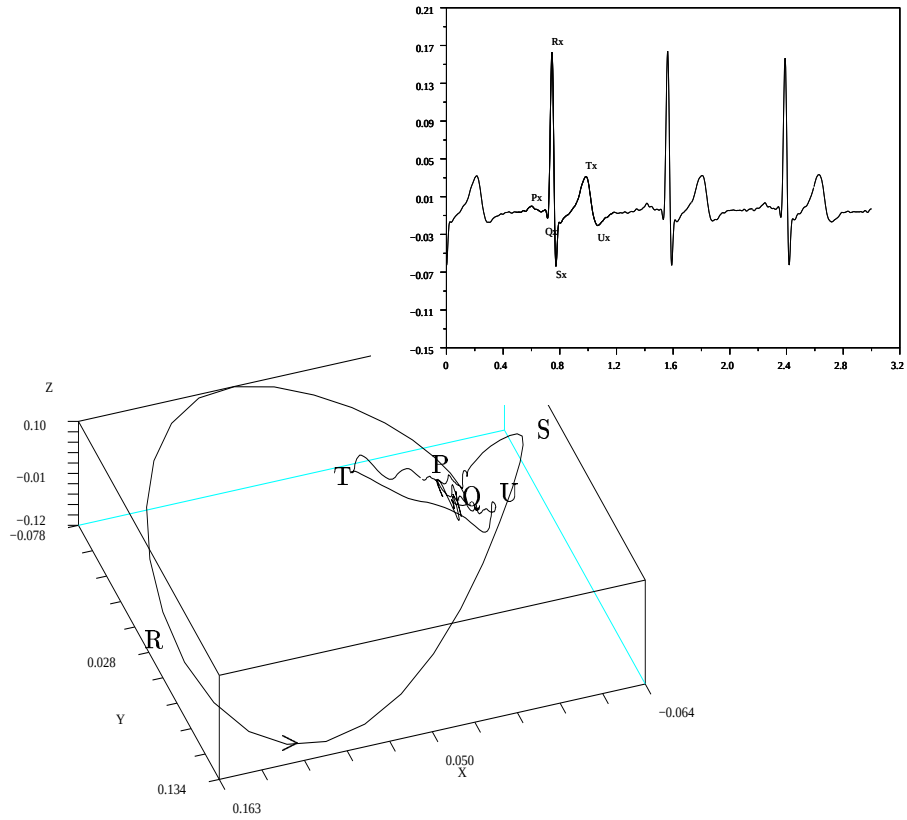

Figure 1 :A one beat VCG and a scalar projection (ECG)

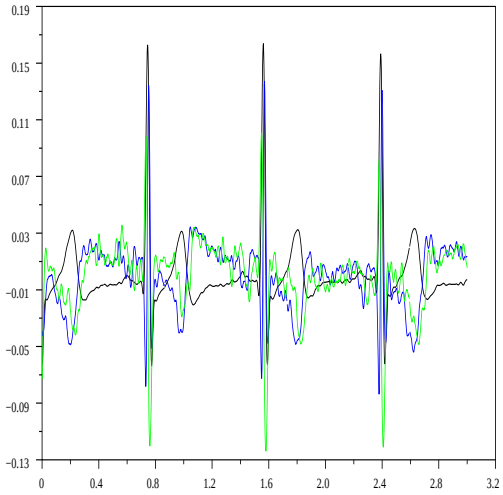

Figure 2

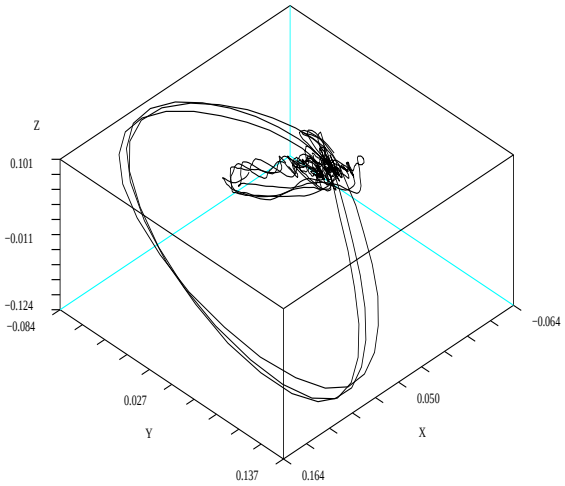

Figure 3

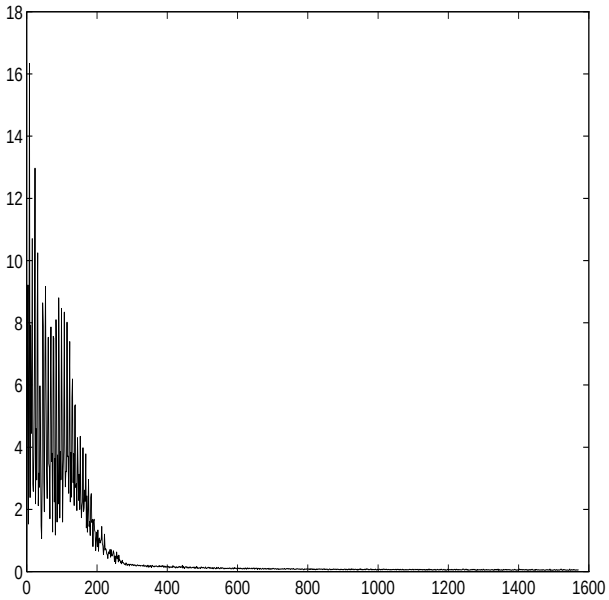

Figure 4

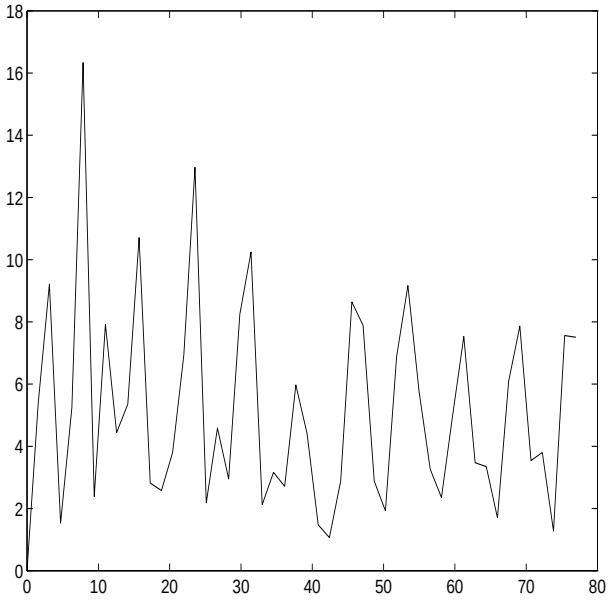

Figure 5

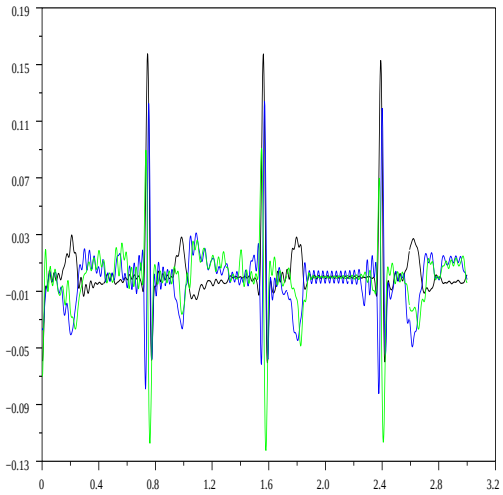

Figure 6

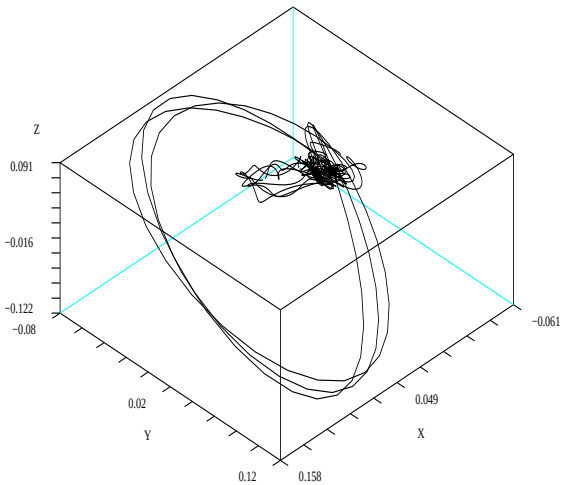

Figure 7

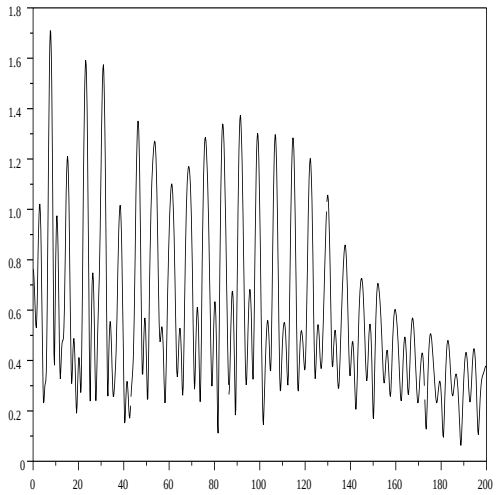

Figure 8

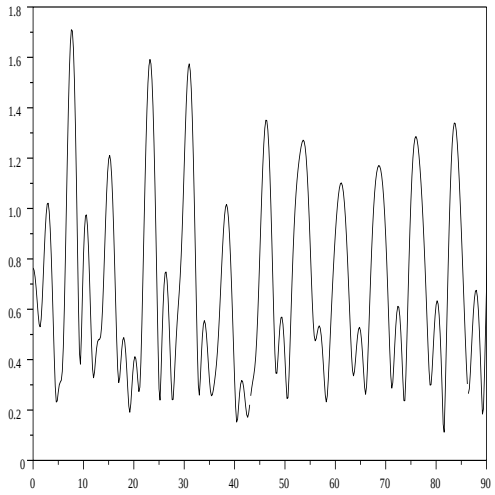

Figure 9

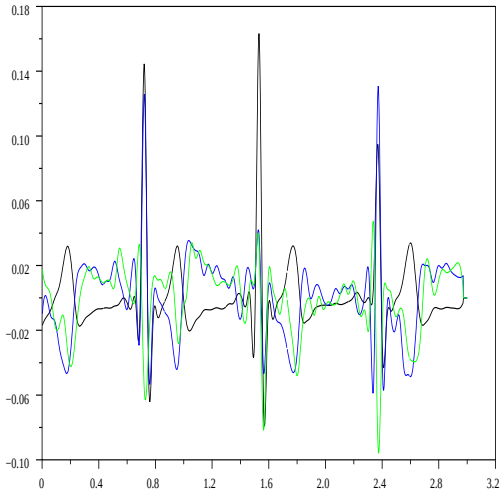

Figure 10

Unit´e de recherche INRIA Lorraine, Technopôle de Nancy-Brabois, Campus scientifique,
615 rue du Jardin Botanique, BP 101, 54600 VILLERS LÈS NANCY
Unit´e de recherche INRIA Rennes, Irisa, Campus universitaire de Beaulieu, 35042 RENNES Cedex
Unit´e de recherche INRIA Rhône-Alpes, 655, avenue de l'Europe, 38330 MONTBONNOT ST MARTIN
Unit´e de recherche INRIA Rocquencourt, Domaine de Voluceau, Rocquencourt, BP 105, 78153 LE CHESNAY Cedex
Unit´e de recherche INRIA Sophia-Antipolis, 2004 route des Lucioles, BP 93, 06902 SOPHIA-ANTIPOLIS Cedex

Éditeur
INRIA, Domaine de Voluceau, Rocquencourt, BP 105, 78153 LE CHESNAY Cedex (France)
ISSN 0249-6399